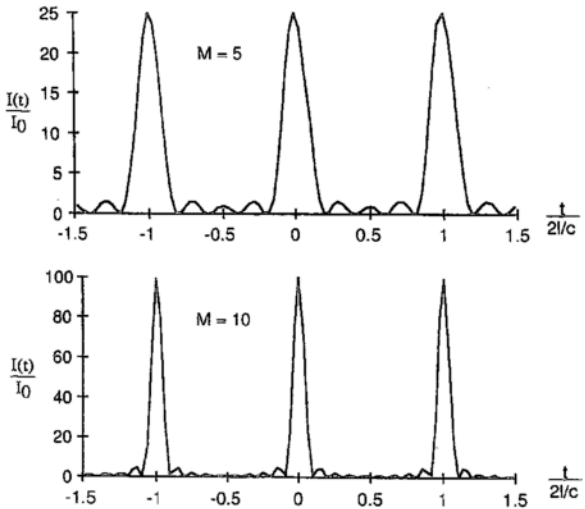

Figure 12.2: *A train of mode-locked pulses as predicted by Eq. (12.5). Top curve is for $M = 5$ and the bottom for $M = 10$. Compare the bottom curve with that in Fig. 12.1.*

because $\mathrm{sinc}(x) = 1$ for $x = 0$. To get an estimate of the width of the pulses, we define the pulse width to be the time between the peak and the first zero. This definition is not exactly full-width at half maximum (FWHM), but very close to it. From Eq. (12.5), the first zero after the peak occurs at $t - t_n = 2\ell/Mc$. Therefore the pulse width τ_p is given by

$$\tau_p = \frac{2\ell}{Mc} \tag{12.7}$$

The average intensity can be determined by integrating over one period as follows:

$$\begin{aligned} I_{\mathrm{av}} &= \frac{1}{T}\int_0^T I(t)\,dt \\ &= \frac{c}{2\ell}\int_0^{2\ell/c} \frac{\mathrm{sinc}^2(Mct/2\ell)}{\mathrm{sinc}^2(ct/2\ell)}\,dt \end{aligned}$$

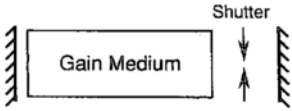

Figure 12.3: *Mode locking can be achieved by introducing a fast shutter in the laser cavity.*

$$= \int_0^1 \frac{\mathrm{sinc}^2(Mt')}{\mathrm{sinc}^2(t')}\,dt'$$
$$\overset{M\gg 1}{\simeq} MI_0, \tag{12.8}$$

where we have defined $t' = ct/2\ell$ in the third equality, and the approximation holds for $M \gg 1$.

Let us consider the example of an Ar^+ laser. The typical laser cavity length is $\ell = 1.5\,\mathrm{m}$ corresponding to $T = 2\ell/c = 10\,\mathrm{ns}$. For far-above threshold pumping, up to 100 modes can oscillate simultaneously. When such a laser is mode locked, we get $\tau = 100\,\mathrm{ps}$ where 1 ps is 10^{-12}s. The shortest pulses to date have been obtained from a dye laser which are only 28 fs long ($1\,\mathrm{fs} = 10^{-15}\,\mathrm{s}$). For a 1.5 m cavity, this would imply that $M = 357,143$. That is, more than three hundred and fifty seven thousand modes are simultaneously locked.

From Eq. (12.7), the average intensity is just M times the intensity of each mode and from Eq. (12.5) the peak intensity is M^2 times the intensity of each mode. Thus for a given average intensity, by locking M modes, the energy of T second time duration gets packed into a short pulse of T/M second duration.

In real lasers, the intensities $\{I_m\}$ of the various oscillating modes are not the same. For example, in a Doppler-broadened laser, they follow a frequency dependence of the kind shown in Fig. 11.4. What effect do the varying intensities have on the mode-locked pulses? It turns out that the pulse width is still determined by the total number of modes whereas the pulse *shape* depends upon the detailed frequency dependence of the mode intensities.

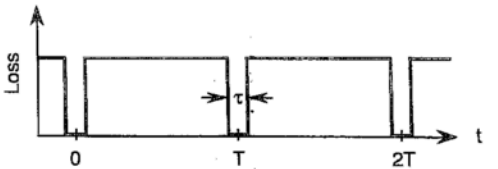

Figure 12.4: *An example time dependence of loss for mode locking via loss modulation.*

12.4 Methods of Mode Locking

In order to mode lock, one somehow needs to force all the lasing modes of a multimode laser to oscillate with the same phase. This can be accomplished by modulating either the gain or the loss of the laser with a period that is equal to the round-trip time of the laser cavity. Since the round-trip time in many lasers is on the order of 10's of nanoseconds, the required modulation frequencies are quite large (100 MHz for 10 ns round-trip time). The gain can be modulated by pulsing the pumping rate W_p. This method is used in mode locking of dye lasers, which are optically pumped. The loss can be modulated by introducing a shutter in the laser cavity (see Fig. 12.3) that opens and closes at the required repetition rate. An acousto-optic modulator is used as a fast shutter in many lasers.

Without going into a detailed mathematical analysis, one can understand graphically how mode locking is achieved by modulating the loss. Assume that the gain is constant whereas the loss is modulated with time dependence as shown in Fig. 12.4. Then a light pulse of duration $\tau_p = \tau$ that arrives at the shutter when the loss is low will pass through the shutter unattenuated. In successive round trips, it will be totally unaware of the presence of the shutter. Light arriving at the shutter at other times, however, will be attenuated. Thus, regardless of the fact that the gain is present at all times, if the loss is modulated with period T, the laser output will be in the form of short pulses of width τ, corresponding to locking of many longitudinal modes.

NORTHWESTERN UNIVERSITY
Department of Electrical Engineering and Computer Science

EECS 379 – Lecture 13

PROPAGATION OF MONOCHROMATIC LIGHT BEAMS

Reading Assignment: GOODMAN – Secs. 2.1 and 2.2.

13.1 Introduction

So far in this course, we have concerned ourselves with the generation of monochromatic light using lasers. Our development has relied on plane waves which have infinite transverse extent. In the remainder of this course, we will study properties of light *beams* with finite transverse extent which are the outputs of real lasers such as a helium-neon laser. We start by learning how light beams propagate in free space.

13.2 Field Normalization

The electric field associated with a monochromatic wave is given by Eq. (2.10) which together with Eqs. (2.13) and (2.19) gives the intensity associated with such a wave at position $\bar{r}$. Since the outputs of most lasers are linearly polarized, and to simplify the notational complexity of the succeeding formulae, we adopt the following scalar wave notation. The electric field associated with a polarized monochromatic wave will be written as

$$u(\bar{r},t) = \mathrm{Re}[U(\bar{r})\exp\{-j2\pi\nu t\}]. \tag{13.1}$$

where, for example, if the field is x polarized $\bar{e}(\bar{r},t) = u(\bar{r},t)\bar{i}_x$. In the above equation $U(\bar{r})$ is a complex function of the spatial coordinate $\bar{r}$ and has been normalized such that the intensity associated with the monochromatic scalar wave is given by

$$I(\bar{r}) = |U(\bar{r})|^2. \tag{13.2}$$

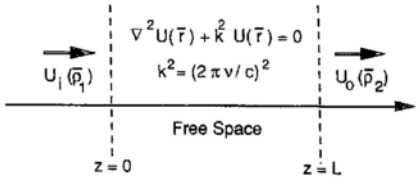

Figure 13.1: *Spatial propagation schematic.*

For a given $\tilde{E}(\bar{r})$, the function $U(\bar{r})$ is easily deduced. The magnitude is obtained using Eqs. (2.13) and (2.19) and the phase is the same as that of $\tilde{E}(\bar{r})$. In terms of $U(\bar{r})$, the Helmholtz equation (2.16) reads

$$\nabla^2 U(\bar{r}) + \frac{\omega^2}{c^2} U(\bar{r}) = 0. \tag{13.3}$$

13.3 Free Space Propagation: Problem Formulation

In most propagation problems of interest, we are concerned with the scenario sketched in Fig. 13.1. The complex field envelope $U(\bar{r})$ associated with a light beam is given at a certain plane, say the $z = 0$ plane, and we need to find the envelope at another plane L meters away. In principle, this can be done by solving the spatial differential equation (13.3) consistent with the boundary condition at $z = 0$ and substituting $z = L$ in the solution so obtained. There is, however, another approach to the solution of this problem that bears a close resemblance to the theory of time invariant linear circuits with which an electrical engineer is intimately familiar with. In this approach, the free space propagation problem can be stated as follows: We are given the input field

$$U_i(\bar{\rho}_1) \equiv U(\bar{r})|_{z=0} = U(x = x_1, y = y_1, z = 0) \tag{13.4}$$

to a system which consists of L meters of free space as shown in Fig. 13.2 and we need to find the output field

$$U_o(\bar{\rho}_2) \equiv U(\bar{r})|_{z=L} = U(x = x_2, y = y_2, z = L) \tag{13.5}$$

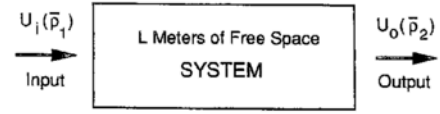

Figure 13.2: *System representation of spatial propagation.*

at $z = L$. Equations (13.4) and (13.5) define the input and output fields in terms of the 2-dimensional position vectors, $\bar{\rho}_1 = (x_1, y_1)$ and $\bar{\rho}_2 = (x_2, y_2)$, spanning the input and output planes at $z = 0$ and $z = L$, respectively. The system of Fig. 13.2 is governed by the Helmholtz equation (13.3) which is linear and shift-invariant as opposed to the linear and time-invariant differential equations describing linear electrical-circuit systems. This analogy is further elaborated on in the following section.

13.4 Time-Invariant Linear Systems

Before discussing 2-dimensional systems, let us recapitulate the methodology of time-domain linear systems. Consider the time-invariant linear system shown in Fig. 13.3 with an input waveform $f(t)$ and an output waveform $g(t')$. Time invariance means that if $g(t')$ is an output to an input $f(t)$, then the output to an input signal $f(t - t_0)$ is given by $g(t' - t_0)$. Similarly, linearity implies that if $g_1(t')$ and $g_2(t')$ are the outputs, respectively, to the inputs $f_1(t)$ and $f_2(t)$, then the output associated with an input signal $af_1(t) + bf_2(t)$ is given by $ag_1(t') + bg_2(t')$ where a and b are arbitrary constants. The above two properties follow from the time-domain linear differential equations describing the time-invariant linear systems.

For time-invariant linear systems, the output $g(t')$ can be obtained from the input $f(t)$ either in the time domain using the system's *impulse response function* $h(t)$ or in the frequency domain using the system's *transfer function* $\tilde{h}(\omega)$. In time domain, the output is given by the convolution integral

$$g(t') = \int dt\, f(t)h(t' - t), \tag{13.6}$$

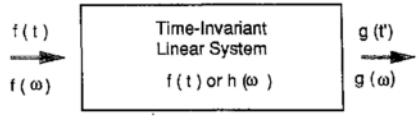

Figure 13.3: *Time domain analog of a linear shift-invariant system.*

whereas in the frequency domain the Fourier transform $\tilde{f}(\omega)$ of $f(t)$, as defined by

$$\tilde{f}(\omega) \equiv \int_{-\infty}^{\infty} dt f(t) \exp(j\omega t), \tag{13.7}$$

is related to the Fourier transform $\tilde{g}(\omega)$ of $g(t')$ via

$$\tilde{g}(\omega) = \tilde{h}(\omega)\tilde{f}(\omega), \tag{13.8}$$

where $\tilde{h}(\omega)$ is the Fourier transform of $h(t)$.

13.5 Two-Dimensional Linear Systems

The spatial system shown in Fig. 13.2 can be analyzed in a similar fashion because the system is linear and shift invariant. In space domain, linearity means that if $U_{o1}(\bar{\rho}_2)$ and $U_{o2}(\bar{\rho}_2)$, respectively, are the output fields associated with the input fields $U_{i1}(\bar{\rho}_1)$ and $U_{i2}(\bar{\rho}_1)$, then the output field associated with the input field $aU_{i1}(\bar{\rho}_1)+bU_{i2}(\bar{\rho}_1)$ is given by $aU_{o1}(\bar{\rho}_2)+bU_{o2}(\bar{\rho}_2)$. This linear property follows from the definitions (13.4) and (13.5) of $U_i(\bar{\rho}_1)$ and $U_o(\bar{\rho}_2)$, respectively, together with the fact that $U(\bar{r})$ is a solution of the Helmholtz equation which is linear. Similarly, shift invariance implies that if $U_o(\bar{\rho}_2)$ is the output field to an input field $U_i(\bar{\rho}_1)$, then the output field associated with the input $U_i(\bar{\rho}_1 - \bar{\rho}_0)$ is given by $U_o(\bar{\rho}_2 - \bar{\rho}_0)$ for any two-dimensional position vector $\bar{\rho}_0$. This property follows from the invariance of the Helmholtz equation under coordinate displacements of the form $\bar{r} \rightarrow \bar{r} - \bar{\rho}_0$.

Similar to the time-invariant linear system case [cf. Eq. (13.6)], the output field of a shift-invariant linear system can be related to the input field via the two-dimensional convolution integral

$$U_o(\bar{\rho}_2) = \int_{-\infty}^{\infty} d\bar{\rho}_1 U_i(\bar{\rho}_1) h(\bar{\rho}_2 - \bar{\rho}_1). \tag{13.9}$$

Here $d\bar{\rho}_1$ is an area element in the $z = 0$ plane given by

$$d\bar{\rho}_1 = dx_1\, dy_1 \tag{13.10}$$

and the limits $(-\infty, \infty)$ indicate a double integral, i.e.,

$$\int_{-\infty}^{\infty} d\bar{\rho}_1 \equiv \int_{-\infty}^{\infty} dx_1 \int_{-\infty}^{\infty} dy_1. \tag{13.11}$$

In Eq. (13.9), $h(\bar{\rho}_2 - \bar{\rho}_1)$ represents the impulse response of the system. An impulse is the field whose value is nonzero only at a point, say $\bar{\rho}_0$ in the input plane. It is represented by a 2-dimensional Dirac delta function $\delta(\bar{\rho}_1 - \bar{\rho}_0)$. Substituting in (13.9), we see that for $U_i(\bar{\rho}_1) = \delta(\bar{\rho}_1 - \bar{\rho}_0)$, $U_o(\bar{\rho}_2) = h(\bar{\rho}_2 - \bar{\rho}_0)$, identifying $h(\bar{\rho}_2 - \bar{\rho}_1)$ to be the impulse response of the shift-invariant linear system. An impulse corresponds to a point source located in the input plane.

In the next Lecture, we will introduce the concepts of 2-dimensional spatial Fourier transforms and obtain a spatial frequency domain solution similar to Eq. (13.8).

NORTHWESTERN UNIVERSITY
Department of Electrical Engineering and Computer Science

Lecture 14 - EECS 379

SPATIAL FOURIER TRANSFORMS AND PLANE WAVES

Reading Assignment: GOODMAN – Secs. 2.1 and 2.2.

14.1 Need for Spatial Fourier Transforms

The convolution integral (13.9), relating the output field $U_o(\bar{\rho}_2)$ of a shift-invariant linear system to its input field $U_i(\bar{\rho}_1)$, is difficult to evaluate in general for an arbitrary $U_i(\bar{\rho}_1)$. In many cases, the output field can be calculated much more easily by working in the Fourier domain. Similar is the case with time-invariant linear systems as pointed out in the previous lecture [cf. Eqs. (13.6)-(13.8)]. To present the Fourier domain method we first need to introduce spatial Fourier transforms. Since the input and output fields are described by 2-dimensional functions, we will need to consider 2-dimensional Fourier transforms.

14.2 2-Dimensional Spatial Fourier Transforms

The spatial Fourier transform of a 2-dimensional function $U(\bar{\rho})$ is defined as:

$$\tilde{U}(\bar{f}) \equiv \int_{-\infty}^{\infty} d\bar{\rho}\, U(\bar{\rho})\, \exp(-j2\pi \bar{f}\cdot\bar{\rho}), \tag{14.1}$$

where the double integral is given by Eq. (13.11), and $\tilde{U}(\bar{f}) = \tilde{U}(f_x, f_y)$ is a 2-dimensional complex function of the spatial frequency $\bar{f} = (f_x, f_y)$ which is itself a 2-dimensional vector in the spatial frequency domain. Since $\exp(-j2\pi \bar{f}\cdot\bar{\rho}) = \exp[-j2\pi(f_x x + f_y y)]$, the above definition is equivalent to the usual Fourier transformation of $U(\bar{\rho}) = U(x, y)$ first with respect to x and then with respect to y (or vice versa). $U(\bar{\rho})$ can be recovered from $\tilde{U}(\bar{f})$ by the inverse Fourier transformation process which is defined via

$$U(\bar{\rho}) \equiv \int_{-\infty}^{\infty} d\bar{f}\, \tilde{U}(\bar{f})\, \exp(j2\pi \bar{f}\cdot\bar{\rho}), \tag{14.2}$$

where, similar to Eq. (13.11), the spatial-frequency domain double integral is given by

$$\int_{-\infty}^{\infty} d\bar{f} \equiv \int_{-\infty}^{\infty} df_x \int_{-\infty}^{\infty} df_y. \tag{14.3}$$

In Homework No. 4 we will evaluate spatial Fourier transforms of some simple functions which will commonly occur in the remainder of this course.

Parseval's Theorem: Using Eqs. (14.1), (14.2), and the fact that I.F.T.$\{\exp(-j2\pi\bar{f}\cdot\bar{\rho}')\} = \delta(\bar{\rho}-\bar{\rho}')$, where I.F.T. stands for inverse Fourier transform (cf. Homework No. 4, Problem No. 1b), it is easily proven that

$$\int_{-\infty}^{\infty} d\bar{f}\,|\tilde{U}(\bar{f})|^2 = \int_{-\infty}^{\infty} d\bar{\rho}\,|U(\bar{\rho})|^2. \tag{14.4}$$

The above equation is a statement of the 2-dimensional Parseval's Theorem.

To simplify the notation, in future we will suppress the overbar on the limits of double integrals. For example, the left member of (14.3) will simply be written as $\int_{-\infty}^{\infty} d\bar{f}$.

14.3 Fourier Domain Propagation Problem

Armed with the definitions of 2-dimensional Fourier Transforms, the Fourier domain equivalent of (13.9) is readily evaluated. Using (14.1) and substituting (13.9), we have

$$\begin{aligned}\tilde{U}_o(\bar{f}) &= \int_{-\infty}^{\infty} d\bar{\rho}_2\, U_o(\bar{\rho}_2)\exp(-j2\pi\bar{f}\cdot\bar{\rho}_2)\\ &= \int_{-\infty}^{\infty} d\bar{\rho}_2 \int_{-\infty}^{\infty} d\bar{\rho}_1\, U_i(\bar{\rho}_1)h(\bar{\rho}_2-\bar{\rho}_1)\exp(-j2\pi\bar{f}\cdot\bar{\rho}_2).\end{aligned}$$

Changing the order of the double integrals and substituting $\bar{\rho}=\bar{\rho}_2-\bar{\rho}_1$ in the above equation

$$\begin{aligned}\tilde{U}_o(\bar{f}) &= \int_{-\infty}^{\infty} d\bar{\rho}_1 U_i(\bar{\rho}_1)\int_{-\infty}^{\infty} d\bar{\rho}_2\, h(\bar{\rho}_2-\bar{\rho}_1)\exp(-j2\pi\bar{f}\cdot\bar{\rho}_2)\\ &= \int_{-\infty}^{\infty} d\bar{\rho}_1\, U_i(\bar{\rho}_1)\int_{-\infty}^{\infty} d\bar{\rho}\, h(\bar{\rho})\exp(-j2\pi\bar{f}\cdot\bar{\rho})\exp(-j2\pi\bar{f}\cdot\bar{\rho}_1)\\ &= \tilde{h}(\bar{f})\,\tilde{U}_i(\bar{f}).\end{aligned} \tag{14.5}$$

Here the spatial transfer function $\tilde{h}(\bar{f})$ is the Fourier transform of the spatial impulse response function $h(\bar{\rho})$. Both $\tilde{h}(\bar{f})$ and $h(\bar{\rho})$ will be evaluated for free-space propagation in the next lecture. Physically, $\tilde{h}(\bar{f})$ represents the amplitude and phase response of the shift-invariant linear system to a complex sinusoid $\exp(j2\pi\bar{f}\cdot\bar{\rho})$ representing a spatially periodic input.

14.4 Simple Solutions of the Helmholtz Equation

The Helmholtz equation (13.3) possesses some simple solutions with clear physical interpretations from which more complicated solutions, commensurate with the given boundary conditions, can be constructed with use of the superposition principal. Before constructing a general solution, let us review a couple of these simple solutions.

14.4.1 Spherical Waves

The normalized complex envelope $U(\bar{r})$ of a spherical wave can be written as

$$U(\bar{r}) = U\frac{\exp(\pm jk|\bar{r}-\bar{r}_0|)}{|\bar{r}-\bar{r}_0|} \tag{14.6}$$

with the + sign representing a diverging spherical wave centered at $\bar{r}_0$ and the − sign describing a spherical wave converging towards $\bar{r}_0$. These are called spherical waves because the surfaces of constant phase are spheres which expand outwards from $\bar{r}_0$ in the former case and inwards towards $\bar{r}_0$ in the latter. This can be shown easily by writing the full spatio-temporal dependence of the real-valued electric field $u(\bar{r},t)$ associated with these waves. Substituting Eq. (14.6) in Eq. (13.1), we obtain

$$u(\bar{r},t) = \frac{|U|}{|\bar{r}-\bar{r}_0|}\cos[2\pi\nu(t\mp|\bar{r}-\bar{r}_0|/c)-\phi], \tag{14.7}$$

where $U = |U|\exp(j\phi)$. Clearly, as t increases, $|\bar{r}-\bar{r}_0|/c$ must increase (for the − sign corresponding to the diverging wave, for example) by the same amount in order for the argument of the cosine function to stay the same (fixed phase). The loci of points $\bar{r}$ for which $|\bar{r}-\bar{r}_0|/c = t$, a constant at a given t, is a sphere of radius ct centered at $\bar{r}_0$. Figure 14.1 shows the cross-section of a diverging spherical wave in the x-z plane. From Eq. (14.6), the intensity of the spherical wave

$$I(\bar{r}) \equiv |U(\bar{r})|^2 = \frac{|U|^2}{|\bar{r}-\bar{r}_0|^2} \tag{14.8}$$

follows an inverse square law. An isotropic point source of geometrical optics located at $\bar{r}_0$ emits diverging spherical waves in the physical-optic description.

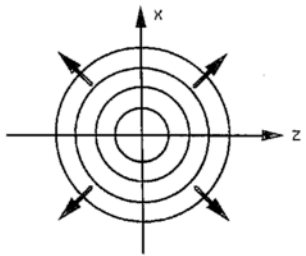

Figure 14.1: *Cross-section of a diverging spherical wave.*

An impulse $U\delta(\bar{\rho}_1 - \bar{\rho}_0)$ can be realized by positioning a point source of amplitude U at $\bar{\rho}_1 = \bar{\rho}_0$ in the input plane ($z = 0$) of an optical system. We assume free space here but it can be any complex system including lenses etc. It will emit spherical waves whose wavefronts at $z = L$ in our system notation can be written as

$$\begin{aligned} U_o(\bar{\rho}) &= U\frac{\exp(jk|\bar{r} - \bar{r}_0|)}{|\bar{r} - \bar{r}_0|} \\ &= U\frac{\exp(jk\sqrt{(x_2 - x_0)^2 + (y_2 - y_0)^2 + z^2})}{\sqrt{(x_2 - x_0)^2 + (y_2 - y_0)^2 + z^2}} \\ &= U\frac{\exp(jkz\sqrt{1 + |\bar{\rho}_2 - \bar{\rho}_0|^2/z^2})}{z\sqrt{1 + |\bar{\rho}_2 - \bar{\rho}_0|^2/z^2}}. \end{aligned} \tag{14.9}$$

Many practical situations of interest are *paraxial* in nature. In such situations we are interested in the field near the optical axis for which $|\bar{\rho}_2 - \bar{\rho}_0| \ll z$. That is, compared to the propagation distance of interest, the transverse location of observation point $\bar{\rho}_2$ is not far from that of the source point $\bar{\rho}_0$. Under this condition, the spherical wavefronts (14.9) can be approximated as

$$\begin{aligned} U_o(\bar{\rho}_2) &= U\frac{\exp(jkz\sqrt{1 + |\bar{\rho}_2 - \bar{\rho}_0|^2/z^2})}{z\sqrt{1 + |\bar{\rho}_2 - \bar{\rho}_0|^2/z^2}} \\ &\simeq U\frac{\exp(jkz)}{z}\exp(jk|\bar{\rho}_2 - \bar{\rho}_0|^2/2z). \end{aligned} \tag{14.10}$$

We will use this approximate form of spherical waves to interpret the impulse response

function $h(\bar{\rho})$ for free-space propagation.

14.4.2 Plane Waves

Monochromatic plane waves, which were introduced in Lecture 2, can be generalized to include evanescent waves (cf. Sec. 3.4). In the normalized scalar-wave notation, a uniform plane wave with wavevector $\bar{k} = k\bar{i}_k$ is represented by

$$U(\bar{r}) = U \exp(j\bar{k} \cdot \bar{r}) \tag{14.11}$$

with $|\bar{k}|^2 = \bar{k} \cdot \bar{k} = (2\pi\nu/c)^2$ and $U = |U| \exp(j\phi)$.

Propagating Waves: When the components k_x, k_y, and k_z of $\bar{k}$ are all real, then (14.11) represents a *propagating* uniform plane wave because the associated real-valued electric field $u(\bar{r}, t)$ takes the following form:

$$u(\bar{r}, t) = |U| \cos[2\pi\nu(t - \bar{r} \cdot \bar{i}_k/c) - \phi], \tag{14.12}$$

showing that the surfaces of constant phase are planes $\perp$ to $\bar{i}_k$. Note that at $z = 0$

$$U(\bar{r}) = U(x, y, z = 0) = U \exp(k_x x + k_y y) \tag{14.13}$$

and $k_x^2 + k_y^2 \leq (2\pi\nu/c)^2$.

Evanescent Waves: In the $U(\bar{r})$ of a plane wave given by (14.11), it is possible that $k_x^2 + k_y^2 > (2\pi\nu/c)^2$. Because $k_x^2 + k_y^2 + k_z^2 = \bar{k} \cdot \bar{k} = (2\pi\nu/c)^2$, this condition implies that $k_z^2 < 0$ or that k_z is imaginary. Writing $k_z = j|k_z|, U(\bar{r})$ of Eq. (14.11) then becomes

$$U(\bar{r}) = U \exp[j(k_x x + k_y y)] \exp(-|k_z| z), \tag{14.14}$$

where

$$|k_z| = \sqrt{(2\pi\nu/c)^2 - k_x^2 - k_y^2}. \tag{14.15}$$

The wave described by Eq. (14.14) is called an *evanescent wave* because it is attenuated for $z > 0$ with an attenuation constant $|k_z|$ given by (14.15). However note that at $z = 0$, the

complex field envelopes $U(\bar{r})$ of both the propagating wave [Eq. (14.11)] and the evanescent wave [Eq. (14.14)] are the same. We will use this fact in the next lecture to derive the general solution of the propagation problem. Finally, the real-valued electric field associated with an evanescent plane wave is given by

$$u(\bar{r},t) = |U| \exp(-|k_z|z) \cos[2\pi\nu(t - \frac{k_x x + k_y y}{2\pi\nu}) - \phi]. \tag{14.16}$$

In the next lecture, we will solve the propagation problem and obtain expressions for $h(\bar{\rho})$ and $\tilde{h}(\bar{f})$.

NORTHWESTERN UNIVERSITY

Department of Electrical Engineering and Computer Science

Lecture 15 – EECS 379

FRESNEL DIFFRACTION

Reading Assignment: GOODMAN – Secs. 3.7 and 4.1.

15.1 Solution of the Propagation Problem

In Lectures 13 and 14, we have defined the free-space propagation problem and developed the methodology that is needed to obtain its solution. We note that our method is not unique; in fact, there are many other ways of solving this problem. Goodman, for example, solves it via a Green's function approach (see Secs. 3.1 through 3.4 of Goodman) that is more suited for physicists whereas our approach appeals more to electrical engineers who are well versed in linear system theory. In summary, we are given the field $U_i(\bar{\rho}_1)$ at $z = 0$ which is propagating nominally along the $+z$ direction and we need to find the field $U_o(\bar{\rho}_2)$ in the $z = L$ plane as shown schematically in Fig. 15.1.

Using the inverse Fourier transform relation (14.2), we can write the input field $U_i(\bar{\rho}_1)$ as

$$U_i(\bar{\rho}_1) = \int_{-\infty}^{\infty} d\bar{f}\, \tilde{U}_i(\bar{f}) \exp(j2\pi \bar{f} \cdot \bar{\rho}_1), \tag{15.1}$$

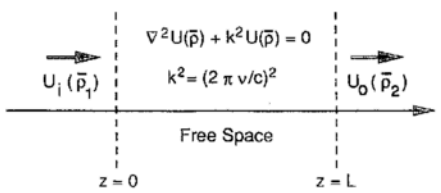

Figure 15.1: *Spatial Propagation Schematic.*

which can be thought of as a superposition of various plane waves

$$\tilde{U}_i(\bar{f}) \exp(j2\pi \bar{f} \cdot \bar{\rho}_1) \tag{15.2}$$

in the $z = 0$ plane. Comparing the above expression with Eq. (14.11), we can identify the wavevectors of the plane waves entering Eq. (15.1) as follows:

$$\bar{k} = (k_x, k_y, k_z) = \begin{cases} \left(2\pi f_x, 2\pi f_y, 2\pi\sqrt{(\nu/c)^2 - f_x^2 - f_y^2}\right), & |\bar{f}| \le 1/\lambda \\ \left(2\pi f_x, 2\pi f_y, 2\pi j\sqrt{f_x^2 + f_y^2 - (\nu/c)^2}\right), & |\bar{f}| > 1/\lambda; \end{cases} \tag{15.3}$$

where k_z is obtained using the dispersion relation $(2\pi\nu/c)^2 = k_x^2 + k_y^2 + k_z^2$ because both Eqs. (14.11) and (15.2) do not involve z. The dispersion relation must always be satisfied by monochromatic light. Also since we assumed that the input is propagating nominally along the $+z$ direction, we have chosen a positive sign for k_z. When $|\bar{f}| \le 1/\lambda$, the identification of (15.2) is with a propagating plane wave because k_x, k_y, and k_z are all real; whereas when $|\bar{f}| > 1/\lambda$, the expression (15.2) represents an evanescent plane wave because k_z is imaginary. Furthermore, that the identification of $\bar{k}$ is correct is guaranteed by the uniqueness theorem.

Now that we have identified the wavevectors of the various plane waves constituting $U_i(\bar{\rho}_1)$, we can find $U_o(\bar{\rho}_2)$ by evaluating each of the component plane waves at $z = L$. For example, the plane wave which at $z = 0$ is given by (15.2) takes the following form at $z = L$ [cf. Eq. (13.5)]:

$$\begin{aligned} & \tilde{U}_i(\bar{f}) \exp[j(k_x x_2 + k_y y_2 + k_z z)]_{z=L} \\ = \; & \tilde{U}_i(\bar{f}) \exp[j(2\pi f_x x_2 + 2\pi f_y y_2)] \exp(jk_z L) \\ = \; & \tilde{U}_i(\bar{f}) \exp(j2\pi \bar{f} \cdot \bar{\rho}_2) \times \begin{cases} \exp\left(jkL\sqrt{1 - |\lambda\bar{f}|^2}\right), & |\bar{f}| \le 1/\lambda \\ \exp\left(-kL\sqrt{|\lambda\bar{f}|^2 - 1}\right), & |\bar{f}| > 1/\lambda; \end{cases} \end{aligned} \tag{15.4}$$

where we have used Eq. (15.3). Summing over all the component plane waves at $z = L$, we get

$$U_o(\bar{\rho}_2) = \int_{-\infty}^{\infty} d\bar{f}\, \tilde{U}_i(\bar{f}) \exp(j2\pi \bar{f} \cdot \bar{\rho}_2) \times \begin{cases} \exp\left(jkL\sqrt{1 - |\lambda\bar{f}|^2}\right), & |\lambda\bar{f}| \le 1 \\ \exp\left(-kL\sqrt{|\lambda\bar{f}|^2 - 1}\right), & |\lambda\bar{f}| > 1 \end{cases}$$

$$\equiv \int_{-\infty}^{\infty} d\bar{f}\, \tilde{U}_i(\bar{f})\, \tilde{h}(\bar{f})\, \exp(j2\pi \bar{f}\cdot \bar{\rho}_2), \tag{15.5}$$

where

$$\tilde{h}(\bar{f}) \equiv \begin{cases} \exp\left(jkL\sqrt{1-|\lambda\bar{f}|^2}\right), & |\lambda\bar{f}| \le 1 \\ \exp\left(-kL\sqrt{|\lambda\bar{f}|^2-1}\right), & |\lambda\bar{f}| > 1. \end{cases} \tag{15.6}$$

Equation (15.5) is in the form of an inverse Fourier transform giving the following Fourier transform of the output field:

$$\tilde{U}_o(\bar{f}) = \tilde{h}(\bar{f})\tilde{U}_i(\bar{f}) \tag{15.7}$$

with $\tilde{h}(\bar{f})$ given by (15.6). Thus, we have solved the propagation problem in the spatial Fourier transform domain. Free-space propagation is equivalent to a shift-invariant linear system whose spatial-frequency response is given by the transfer function $\tilde{h}(\bar{f})$ of Eq. (15.6).

15.2 Paraxial Approximation

From Eq. (14.4), the spatial impulse response function $h(\bar{\rho})$ is the inverse Fourier transform of the spatial transfer function $\tilde{h}(\bar{f})$. It is difficult to evaluate the former in general because of the discontinuity in the latter at $|\bar{f}| = 1/\lambda$. However, in most practical situations, the evanescent waves, which do not carry any power in the $+z$ direction, are of no interest. Moreover, in many applications such as: i) optical communications where $U_i(\bar{\rho}_1)$ is the field emitted by the transmitter and $U_o(\bar{\rho}_2)$ is that incident on the receiver, ii) coherent imaging where $U_i(\bar{\rho}_1)$ is the source field and $U_o(\rho_2)$ is the image field, iii) optical signal processing where $U_i(\bar{\rho}_1)$ is the input signal to the optical processor and $U_o(\bar{\rho}_2)$ is the corresponding output; $U_i(\bar{\rho}_1)$ is such that the corresponding Fourier function $\tilde{U}_i(\bar{f})$ is bounded from above at a spatial frequency $|\bar{f}|_{\max} = f_0$ which is much less than $1/\lambda$, i.e., $|\tilde{U}_i(\bar{f})| = 0$ for $|\bar{f}| > f_0 \ll 1/\lambda$. From Parseval's theorem [cf. Eq. (14.4)], the input power P_i is then carried by spatial frequencies whose magnitudes are much smaller than $1/\lambda$:

$$\begin{aligned} P_i &\equiv \int_{-\infty}^{\infty} |U_i(\bar{\rho}_1)|^2\, d\bar{\rho}_1 \\ &= \int_{-\infty}^{\infty} |\tilde{U}_i(\bar{f})|^2\, d\bar{f} \simeq \int_{|\bar{f}|\le f_0} |\tilde{U}_i(\bar{f})|^2\, d\bar{f}. \end{aligned} \tag{15.8}$$

Under these circumstances, i.e.. when $|\lambda \bar{f}|_{\max} \ll 1$, we can approximate $\tilde{h}(\bar{f})$ of (15.6) by

$$\begin{aligned} \tilde{h}(\bar{f}) &\simeq \exp\left[jkL\left(1-|\lambda\bar{f}|^2\right)^{1/2}\right] \\ &\simeq \exp\left[jkL\left(1-|\lambda\bar{f}|^2/2\right)\right] \\ &= \exp(jkL)\exp\left(-j\pi\lambda L|\bar{f}|^2\right), \end{aligned} \tag{15.9}$$

where first we have thrown away the evanescent part, and second, kept only the first two terms in the Taylor series expansion of the exponent. This is known as the *parazial approximation* and is very accurate in the examples cited above. Under this approximation, the free-space transfer function is a simple Gaussian function of spatial frequency. From Eq. (15.3), $f_x = k_x/2\pi$ and $f_y = k_y/2\pi$, implying that $|\lambda\bar{f}| \ll 1$ is equivalent to $|\bar{k}_\perp| \ll 2\pi/\lambda = k$ where $\bar{k}_\perp \equiv (k_x, k_y, 0)$ is the component of $\bar{k}$ perpendicular to z. Thus the paraxial approximation, as the name justifies, has the following physical interpretation: The plane waves that constitute $U_i(\bar{\rho}_1)$ are all such that they propagate almost along the $+z$ direction.

15.3 Spatial Impulse Response Function

Under paraxial approximation, using Eq. (15.9)

$$\begin{aligned} h(\bar{\rho}) &= \int_{-\infty}^{\infty} d\bar{f}\, \tilde{h}(\bar{f}) \exp(j2\pi\bar{f}\cdot\bar{\rho}) \\ &= \int_{-\infty}^{\infty} d\bar{f}\, \exp(jkL)\exp\left(-j\pi\lambda L|\bar{f}|^2\right)\exp(j2\pi\bar{f}\cdot\bar{\rho}) \\ &= \frac{\exp(jkL)}{j\lambda L}\exp\left(jk|\bar{\rho}|^2/2L\right). \end{aligned} \tag{15.10}$$

Here, the last equality is obtained via the following Fourier transform relationship for 2-dimensional Gaussians (cf. Homework No. 5. Problem No. 1):

$$\text{F.T.}\left\{\frac{\exp(-|\bar{\rho}|^2/2v^2)}{2\pi v^2}\right\} = \exp\left[-(2\pi v)^2|\bar{f}|^2/2\right] \tag{15.11}$$

for $\text{Re}(v^2) \geq 0$. Thus, we have shown that under paraxial approximation, the free-space propagation problem is equivalent to a shift-invariant linear system whose impulse response is given by $h(\bar{\rho})$ of Eq. (15.10).

In physical optics, an impulse is nothing but a point source located in the input plane. In Sec. (14.4.1), we saw that such a point source emits spherical waves whose wavefronts, under paraxial conditions, are given by Eq. (14.10). Comparing Eq. (15.10) with (14.10), we see that $h(\bar{\rho})$ is nothing but a description of how spherical waves pass through the optical system. The two equations are identical if the amplitude $U(\bar{\rho}_1)$ of the input spherical waves in (14.10) is taken to be $(-j/\lambda)U_i(\bar{\rho}_1)$ [cf. Eq. (15.12) below].

15.4 Space-Domain Solution of the Propagation Problem

Substituting $h(\bar{\rho})$ of Eq. (15.10) into Eq. (13.9), we obtain

$$\begin{aligned} U_o(\bar{\rho}_2) &= \int_{-\infty}^{\infty} d\bar{\rho}_1\, U_i(\bar{\rho}_1)\, h(\bar{\rho}_2 - \bar{\rho}_1) \\ &= \int_{-\infty}^{\infty} d\bar{\rho}_1\, U_i(\bar{\rho}_1)\, \frac{\exp(jkL)}{j\lambda L} \exp\left(jk|\bar{\rho}_2 - \bar{\rho}_1|^2/2L\right) \\ &= \frac{\exp(jkL)}{j\lambda L} \int_{-\infty}^{\infty} d\bar{\rho}_1\, U_i(\bar{\rho}_1) \exp\left(jk|\bar{\rho}_2 - \bar{\rho}_1|^2/2L\right), \end{aligned} \tag{15.12}$$

which is known as the *Fresnel diffraction formula*. It gives, under paraxial approximation, the output field $U_o(\bar{\rho}_2)$ in terms of the input field $U_i(\bar{\rho}_1)$ as a 2-dimensional integral over the input plane.

In the next lecture, we will study Gaussian beams of light which maintain their form under Fresnel diffraction (paraxial propagation).

NORTHWESTERN UNIVERSITY
Department of Electrical Engineering and Computer Science

Lecture 16 – EECS 379

EXAMPLE OF FRESNEL DIFFRACTION: GAUSSIAN BEAMS OF LIGHT

Reading Assignment: YARIV – Secs. 2.4 and 2.5.

16.1 Gaussian Beams

The idealized theory of a generic laser that we developed in Lectures 7 and 8 was based on plane waves. The resulting output is also a plane wave apertured by the output mirror. Real lasers, however, do not emit plane waves: the output of most lasers are Gaussian beams of light. In the normalized scalar-wave notation, the spatial profile of the complex envelope of a monochromatic Gaussian beam propagating along the $+z$ direction can be written as:

$$U(\bar{r}) = U(\bar{\rho}) \exp(jkz) \tag{16.1}$$

with

$$U(\bar{\rho}) = \sqrt{\frac{P_t}{\pi a^2}} \exp(jk|\bar{\rho}|^2/2q). \tag{16.2}$$

Here q is a complex beam parameter that describes the phase radius of curvature R and the intensity radius a of the Gaussian beam via

$$\frac{1}{q} = \frac{1}{R} + \frac{j}{ka^2}. \tag{16.3}$$

In general, both a and R, and hence q, are functions of z.

Taking the modulus square of Eq. (16.2) and using (16.3), the spatial profile of the intensity of the Gaussian beam is given by

$$I(\bar{\rho}) = |U(\bar{\rho})|^2 = \frac{P_t}{\pi a^2} \exp(-|\bar{\rho}|^2/a^2), \tag{16.4}$$

which is a 2-dimensional Gaussian in x and y, thus justifying the name for these beams. In Fig. 16.1, we have plotted the intensity variation along the x direction. Because Eq. (16.4)

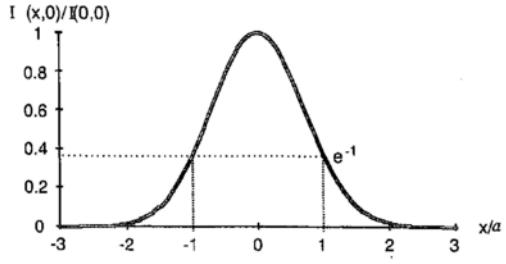

Figure 16.1: *Intensity profile of a Gaussian beam.*

is radially symmetric, similar intensity variation occurs along any radial direction in the x-y plane. Also the intensity at $|\bar{\rho}| = a$ drops to e^{-1} of its peak value at $|\bar{\rho}| = 0$. Therefore, we call a to be the intensity radius of the Gaussian beam. Integrating $I(\bar{\rho})$ over the x-y plane, we get

$$\int_{-\infty}^{\infty} I(\bar{\rho})\, d\bar{\rho} = \int_{-\infty}^{\infty} d\bar{\rho}\, \frac{P_t}{\pi a^2} \exp(-|\bar{\rho}|^2/a^2) = P_t, \tag{16.5}$$

which identifies P_t to be the total power transported by the Gaussian beam in the $+z$ direction. Substituting (16.2) and(16.3) in (16.1), we see that the phase part of $U(\bar{r})$ is given by

$$\exp(jk|\bar{\rho}|^2/2R) \exp(jkz).$$

The above expression is of the same form as the phase part of a spherical wave in the paraxial limit [cf. Eq. (14.10)]. Comparing the two we identify R to be the radius of curvature of the spherical wavefronts associated with the Gaussian beam.

16.2 Free-Space Propagation of Gaussian Beams

It can be shown by direct substitution that a Gaussian beam (16.2) satisfies the Fresnel diffraction formula (15.12) derived in the previous Lecture. We will leave the proof as a homework exercise. Here we tackle the problem of free-space Gaussian-beam propagation in the spatial-frequency domain using the transfer function approach. Specifically, we need to

find the output field $U_o(\bar{\rho}_2)$ at $z = L$ for an input field $U_i(\bar{\rho}_1)$ describing a Gaussian beam at $z = 0$. Writing $q(z = 0)$ as q_0 and $a(z = 0)$ as a_0, from Eq. (16.2) we have

$$U_i(\bar{\rho}_1) = \sqrt{\frac{P_t}{\pi a_0^2}} \exp(jk|\bar{\rho}_1|^2/2q_0), \tag{16.6}$$

whose Fourier transform is also a Gaussian in the spatial-frequency domain. It is easily obtained using formula (15.11) to be

$$\begin{aligned} \tilde{U}_i(\bar{f}) &= \int_{-\infty}^{\infty} d\bar{\rho}_1 \sqrt{P_t/\pi a_0^2} \exp(jk|\bar{\rho}_1|^2/2q_0) \exp(-j2\pi \bar{f} \cdot \bar{\rho}_1) \\ &= \sqrt{P_t/\pi a_0^2}\, j\lambda q_0 \exp(-j\pi\lambda q_0 |\bar{f}|^2). \end{aligned} \tag{16.7}$$

The Fourier transform of the output field is obtained from that of the input by multiplying the latter with the free-space spatial transfer function $\tilde{h}(\bar{f})$ [cf. Eqs. (14.5) and (15.7)]. $\tilde{h}(\bar{f})$ was derived under the paraxial approximation in Eq. (15.9) and is given by

$$\tilde{h}(\bar{f}) = \exp(jkL) \exp(-j\pi\lambda L|\bar{f}|^2) \tag{16.8}$$

for L meters of propagation. Substituting (16.7) and (16.8) in (15.7), we get

$$\begin{aligned} \tilde{U}_o(\bar{f}) &= \tilde{h}(\bar{f})\, \tilde{U}_i(\bar{f}) \\ &= \sqrt{P_t/\pi a_0^2}\, j\lambda q_0 \exp(jkL) \exp[-j\pi\lambda(q_0 + L)|\bar{f}|^2] \\ &= \sqrt{P_t/\pi a_0^2}\, \frac{q_0}{q_0 + L} \exp(jkL)\, j\lambda(q_0 + L) \exp[-j\pi\lambda(q_0 + L)|\bar{f}|^2], \end{aligned} \tag{16.9}$$

where in the last equality we have multiplied the numerator and the denominator by $(q_0 + L)$. The above equation is of the same form as the Fourier transform of the input field. In analogy with the Fourier transform pair (16.6) and (16.7), we can immediately write the inverse Fourier transform of $\tilde{U}_o(\bar{f})$ as

$$\begin{aligned} U_o(\bar{\rho}_2) &= \sqrt{P_t/\pi a_0^2}\, \frac{q_0}{q_0 + L} \exp(jkL) \exp[jk|\bar{\rho}_2|^2/2(q_0 + L)] \\ &= \sqrt{P_t/\pi a_0^2}\, \frac{q_0}{q(L)} \exp(jkL) \exp[jk|\bar{\rho}_2|^2/2q(L)], \end{aligned} \tag{16.10}$$

where

$$q(L) = q_0 + L. \tag{16.11}$$

Thus we see that under paraxial propagation, a Gaussian beam maintains its form. It stays as a Gaussian beam except that its q parameter changes according to Eq. (16.11). This result is a direct consequence of the Gaussian structure of the free-space transfer function $\tilde{h}(\tilde{f})$ under the paraxial condition.

Equation (16.11) describes how the phase radius of curvature R and the intensity radius a of the Gaussian beam change as it propagates through free space. Using (16.3), Eq. (16.11) can be decomposed into equations for $a(L)$ and $R(L)$ as follows:

$$\begin{aligned}\frac{1}{q(L)} &\equiv \frac{1}{R(L)} + \frac{j}{ka^2(L)} = \frac{1}{q_0 + L} = \frac{1}{q_0}\,\frac{1}{1 + L/q_0} \\ &= \frac{1/R_0 + j/ka_0^2}{(1 + L/R_0) + jL/ka_0^2}.\end{aligned}$$

Comparing the real and imaginary parts on both sides of the above equation, we immediately obtain

$$R(L) = L\frac{[(1 + L/R_0)^2 + \Omega_L^{-2}]}{[(1 + L/R_0)L/R_0 + \Omega_L^{-2}]}, \tag{16.12}$$

$$a(L) = a_0[(1 + L/R_0)^2 + \Omega_L^{-2}]^{1/2}, \tag{16.13}$$

where $\Omega_L \equiv ka_0^2/L$ is a dimensionless parameter. Thus, we see that both the phase radius of curvature R and the intensity radius a vary in a complicated way as the Gaussian beam propagates through free space. In the next lecture, we will examine their behavior in some detail for a couple of scenarios that commonly arise in the laboratory. Also, we will describe the physical significance of the dimensionless parameter Ω_L.

Let us now go back to Eq. (16.10) and simplify the expression for $U_o(\bar{\rho}_2)$. Once again $q_0/q(L)$ can be simplified by decomposing it into an amplitude and a phase part. Using (16.3)

$$\begin{aligned}\frac{q_0}{q_0 + L} = \frac{1}{1 + L/q_0} &= \frac{1}{(1 + L/R_0) + jL/ka_0^2} \\ &\equiv [(1 + L/R_0)^2 + \Omega_L^{-2}]^{-1/2}\exp[j\Theta(L)],\end{aligned} \tag{16.14}$$

where

$$\Theta(L) = -\tan^{-1}[\frac{\Omega_L^{-1}}{1 + L/R_0}]. \tag{16.15}$$